Performance Analysis of High Speed Power Quality Disturbance Recognition Scheme for Static Transfer Switch Application

RAMESH PACHAR[1]
Elect. Engg. Department,
SKIT, M&G, Jaipur-302025
INDIA
hodee@mail.skit.ac.in,
http://www.skit.ac.in,

HARPAL TIWARI[2]
Elect. Engg. Department,
MNIT, Jaipur-302025
INDIA
harpaltiwari@yahoo.co.in
http://www.mnit.ac.in

RAMESH.C.BANSAL[3]
School of Elect. Engg. & I T,
University of Queensland,
AUSTRALIA
bansal_r@usp.ac.fj
www.usp.ac.fj

Abstract: - The static Transfer Switch (STS) is a network reconfiguring device and is used for power quality improvement of sensitive loads. It selects, at high speeds, between two or more sources of power and provides the best available power to the sensitive load. This paper presents fundamentals of solid state STS with a detailed emphasis on power quality disturbance recognition scheme, as it is responsible for fast and accurate detection of disturbances, thereby ensuring healthy transfer of load to an alternate source. Extensive simulations are carried out for investigating the performance of rather commonly employed detection scheme. The behavior of detection scheme is analyzed against various types of disturbance scenarios including system transients.

Key Words: - Power Quality, Static Transfer Switch, Detection Scheme, Transfer Time, Sensitive Loads, Custom Power Devices.

1 Introduction

In past few years power quality has gained a lot of importance among researchers due to its implications on sensitive residential and industrial loads. Availability of semiconductor devices at low and medium voltage levels has lead to development of *custom power devices* which provides much faster and efficient control in distribution system for network compensation and reconfiguration applications[1]. A STS is a network reconfiguration device and it is widely used for power quality improvement of sensitive loads. It does so by flexibly changing the distribution configuration [1]-[5]. STS basically comprises of two sources namely preferred source and alternate source, a control logic scheme and a sensitive load whose protection is desired against the power quality disturbances. Performance of a STS system is analyzed with respect to transfer time. With GTO based STS systems almost constant transfer time can be obtained and the total load transfer time can be reduced considerably [8]. A faultless detection scheme is of utmost necessity for proper and reliable functioning of a STS system [9]-[11]. The applied detection scheme must be able to provide faster detection of disturbances and this should be achieved with a high degree of accuracy. The single line diagram and structural topology of a STS scheme are shown in Fig.1and Fig.2 respectively. A detailed description of operational concept and basics of control philosophy are presented in this section. Section 2 briefly describes the principle of operation of a STS system [7]. Section 3 discusses the control strategy employed for detection of power quality problem. Section 4 describes the variations in detection time with its dependency on (1) the type (single-phase/two-phase/three-phase) and degree of disturbance and (2) point-on-wave where initiation of the fault/sag has occurred. The impact of switching transients on the performance of detection scheme for ambiguous detection and transfer is also investigated. Derived conclusions are presented in section 5. Detailed simulations are carried out for a three-phase STS system feeding a sensitive R-L load. The simulation model is developed using the simulink and simpowersystems utilities of MATLAB.

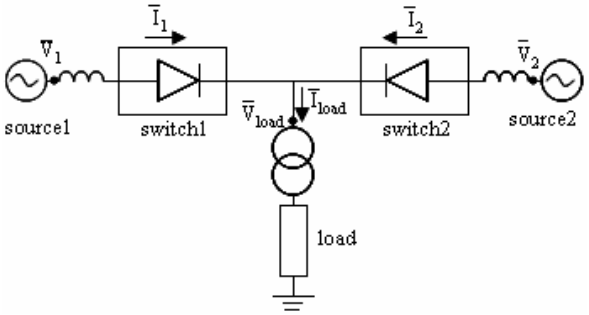

Fig.1: Single Line Diagram of a STS scheme

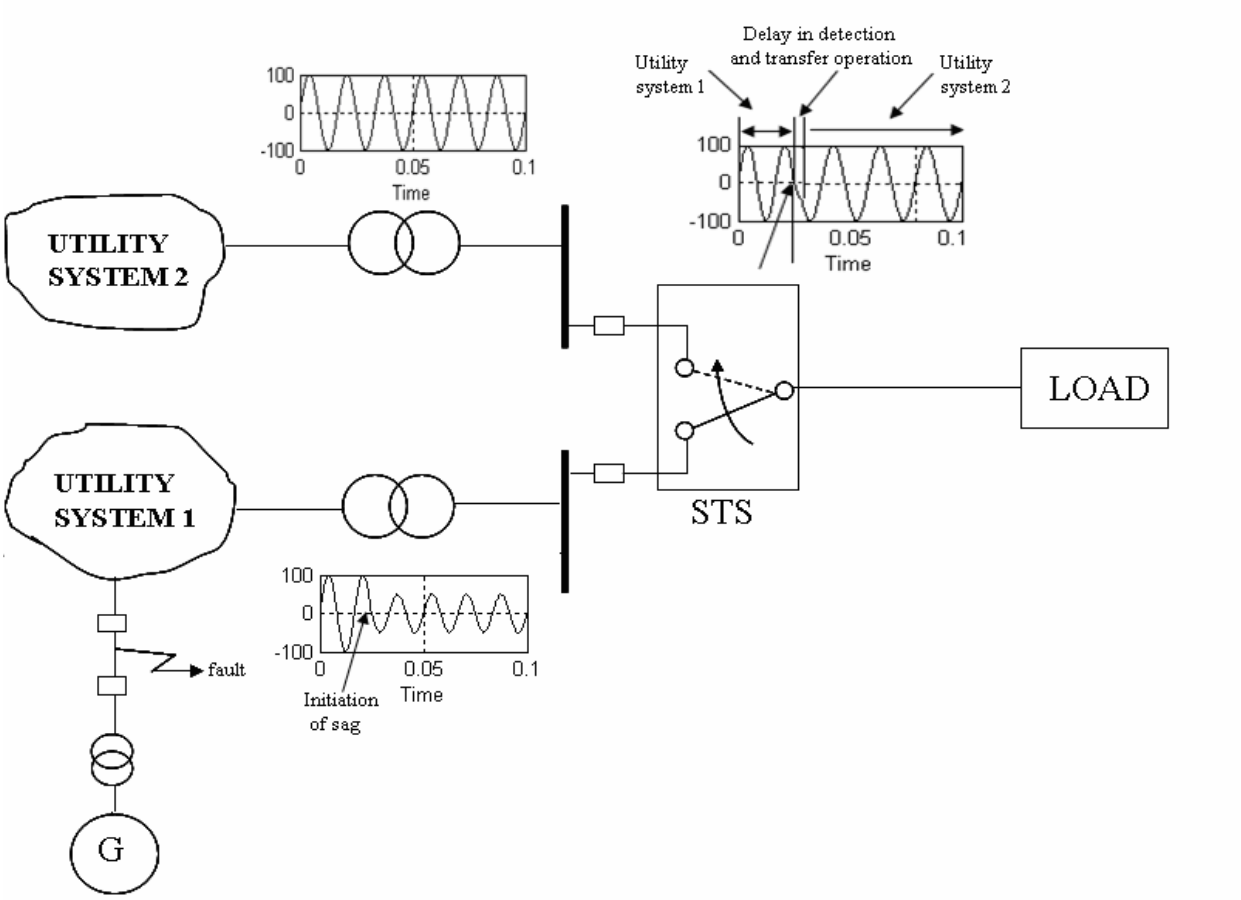

Fig.2: Basic Structural and Switching Concept of STS System

1.1 Operational Concept of STS System

Custom power devices have gained a lot of interest among researchers due to their inherent advantages over electromechanical devices. The term custom power pertains to the use of solid state devices for compensation and restructuring of power system distribution networks. A STS system is a network reconfiguring device and is used for power quality improvement of sensitive loads.

Figure 2 shows the basic structure and concept of a static transfer switch application. STS system is composed of a pair of antiparallel SCR thyristors/Gate turn off devices and enables seamless transfer of energy from a preferred source to an alternate source so as to ensure interruption free power supply to the sensitive load and hence improves the power quality. Figure 2 illustrates the phenomena of load transfer when generator of utility system1 is subjected to a fault leading to sag in source voltage. Control strategy takes necessary action by identifying the power quality problem and in turn transferring the load to utility system2. Time involved in transfer of load has two components namely *detection time* and *load transfer time*. The sum of these two is designated as the total *transfer time*. Recent advances in semiconductor technology have encouraged the applications of such devices in medium voltage systems. The circuit representation of a single phase STS system employed with GTO switches is shown in Figure 3. It consists of two feeders (feeder 1 and feeder 2) and a load which can be connected to any of them via switch1 or switch2. Preferred source is one which exhibits better power quality as compared to the other one (alternate source).

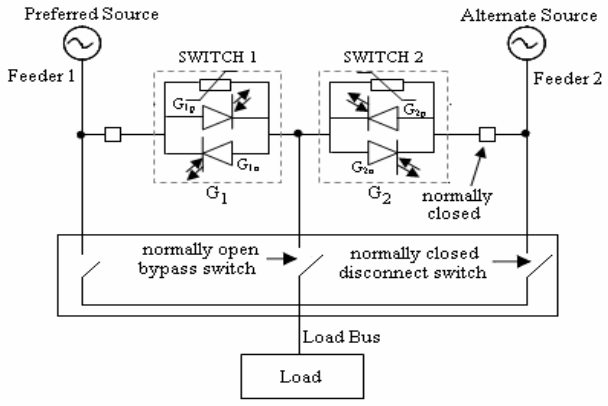

Fig.3: Single Phase schematic of STS System

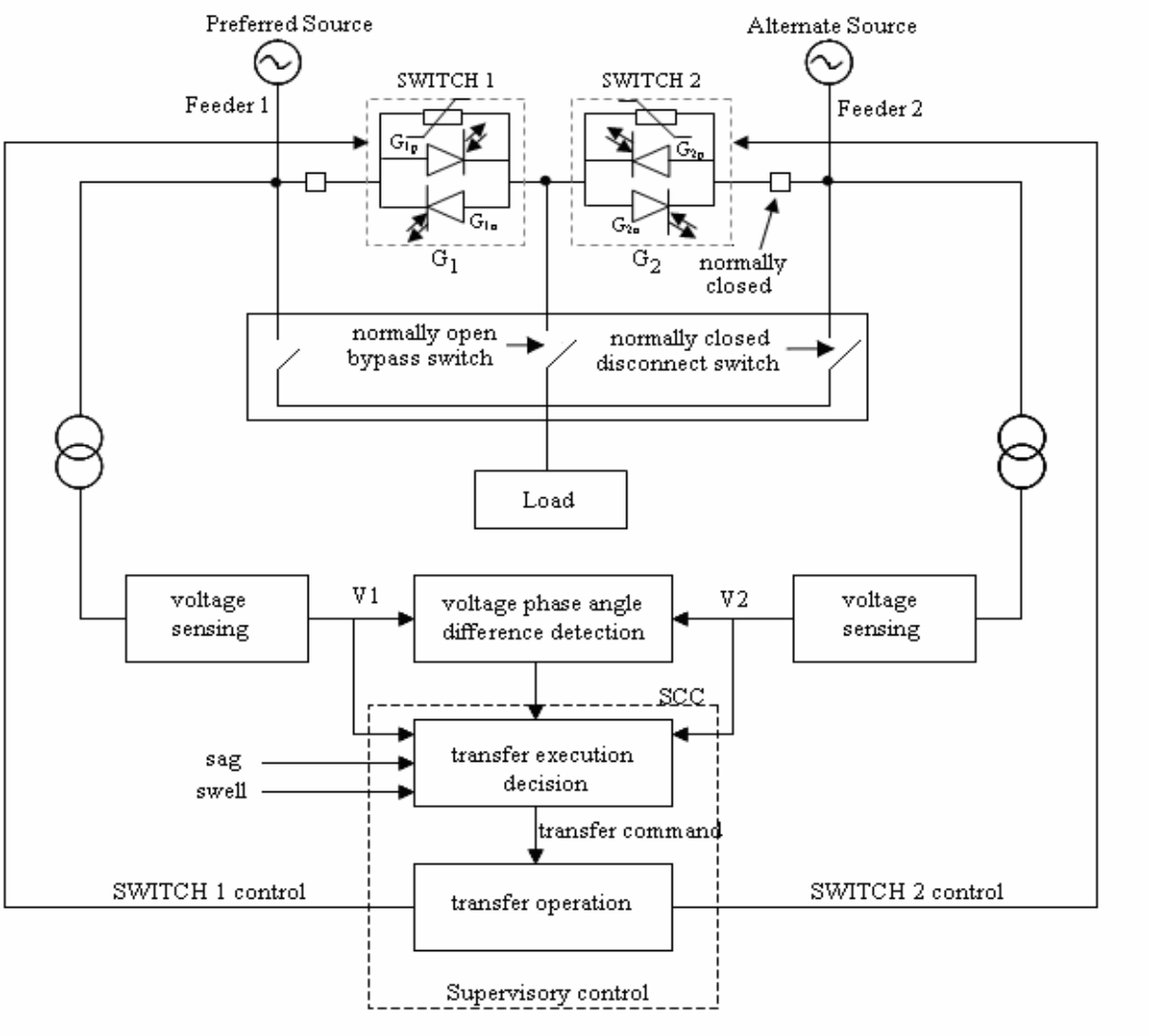

Fig.4: Block Diagrammatic Representation of Control Scheme

1.2 Basics of Control Philosophy

Control scheme is shown in Figure 4. Major components of control scheme are voltage detection scheme and firing logic. Voltage scheme continuously monitors the power quality of both the sources. This includes determination of voltage sags/swells in the supplying source. Firing logic is responsible for generation of proper firing sequence for any of the two switches during normal operation of STS.

Voltage sensing scheme accept inputs from both sources via potential transformers (PT's). The V1 and V2 are the two outputs of sensing schemes and are further processed (discussed in detail in section 3) for identifying the deviation from the nominal value of rms voltage. This helps in determining the healthier source at a given time. At the same time voltage phase angle difference in both feeders is also detected which helps in deciding exact instant of shifting the firing pulses from one switch (corresponding to unhealthy source) to the other (switch corresponding to healthier source). Output of voltage detection and phase angle difference detection scheme is passed to transfer execution decision block. Depending upon the status of input voltages and phase angle difference, the instant of transferring the load to other feeder is decided. Output of this block is a transfer signal (usually a binary signal) which initiates the transfer operation. A High (1) status indicates abnormal condition of supplying feeder whereas low (0) value indicates normal (healthy) condition of source supplying the load. The transfer operation block is responsible for removing the firing pulses from one switch and to trigger the SCR /GTO switch corresponding to healthy source. Section 3 describes, in detail the operation of control strategy employed in three-phase GTO based STS.

2 Principle of Operation

The basic structure of a three-phase STS system is shown in Fig.5. The system is composed of:

• A load which is sensitive to variations of utility supply,

• Two independent sources one of which is the preferred one and the other is the alternate one,

• Two GTO blocks G_1 and G_2 which connect the load to the power sources and

• Control logic to monitor voltage quality of both sources, detect voltage fluctuations in the system (detection process), compare the two sources, and perform a load transfer from one source to the other one if needed. STS blocks G_1 and G_2 each contain three modules corresponding to the three phases of the system. Each GTO module includes two anti-parallel GTO switches (G_{1p}/G_{1n} and G_{2p}/G_{2n}). Under normal operating conditions, i.e., when the preferred source meets load voltage requirements, the control logic trigger only the thyristors of G_1. If the preferred source cannot meet voltage requirements, the control logic will transfer the load to the alternate source if it is in a better condition than the preferred one. This is achieved by removing gating signals from thyristors G_1 and triggering thyristors of switch G_2. In case of voltage recovery, the load is transferred back to the preferred source. Input signals in Fig. 2 are those required for controlling the STS operation.

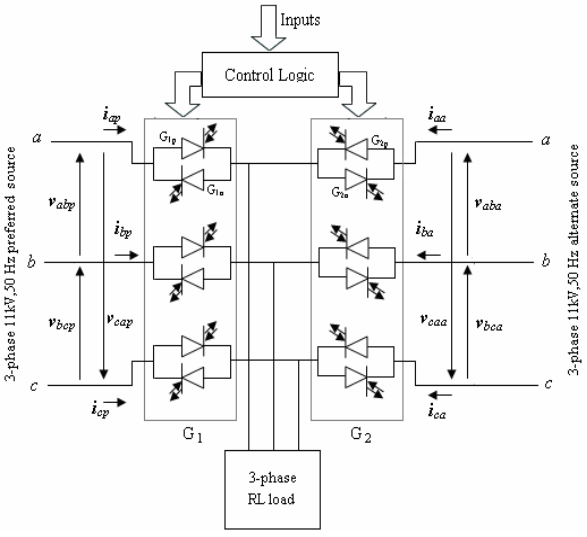

Fig.5: Power circuit of a three-phase STS system

3 Control Strategy

Fig.6 refers to a rather common detection technique based on Park transformation. The instantaneous three-phase voltages $V_a(t), V_b(t), V_c(t)$ are transformed into a fixed two-axis coordinate system, called αβ-

$$\begin{bmatrix} V_\alpha(t) \\ V_\beta(t) \\ V_0(t) \end{bmatrix} = \sqrt{\frac{2}{3}} \begin{bmatrix} 1 & -\frac{1}{2} & -\frac{1}{2} \\ 1\ 0 & \frac{\sqrt{3}}{2} & \frac{-\sqrt{3}}{2} \\ \frac{1}{\sqrt{2}} & \frac{1}{\sqrt{2}} & \frac{1}{\sqrt{2}} \end{bmatrix} \begin{bmatrix} V_a(t) \\ V_b(t) \\ V_c(t) \end{bmatrix} \text{------(1)}$$

coordinate system, as in equation *(1)*; where $V_0(t)$ is the zero-sequence voltage component, which will no longer be considered. The voltage vector thus obtained is further transformed into a rotating *dq*-coordinate system, according to the equation:

$$\underline{V}^{(dq)}(t) = e^{-j\theta(t)} \underline{V}^{(\alpha\beta)}(t) \text{------(2)}$$

Where $\theta(t)$ is the transformation angle, calculated as

$$\theta(t) = \theta(0) + \int_0^t \omega(\xi) d\xi \text{------(3)}$$

Finally the amplitude of supply vector is calculated as indicated by equation no. *(4)* and is

$$V_{dq} = \sqrt{V^2{}_d + V^2{}_q} \text{------(4)}$$

compared with the reference value to identify a disturbance. V_{dq} is passed through a suitable second order filter to attenuate the impact of natural power system transients hence preventing the faulty operation of the STS system. The output of detection scheme is a binary signal. A low (0) value indicates healthy condition of preferred source whereas high (1) value indicates a disturbance and initiates the transfer process.

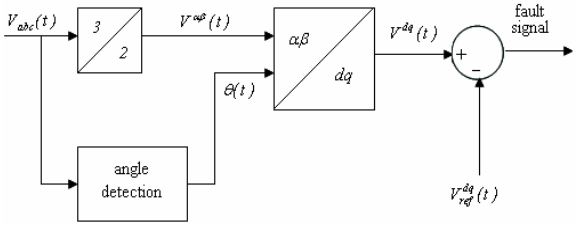

Fig.6: Fault detection scheme

An interval of 4ms is thus often claimed as maximum time in which transfer of the load to the alternate supply is completed. However a careful analysis indicates that such a small duration cannot be ensured in all types of disturbances due to the dependency of detection time on type of disturbance, on the point-on-wave where fault/disturbance has initiated, on the response of detection scheme against switching transients and on actual operating condition of the power system when transfer is initiated. In addition to this transfer time transfer time depends on detection scheme and on type of switching devices used [7].

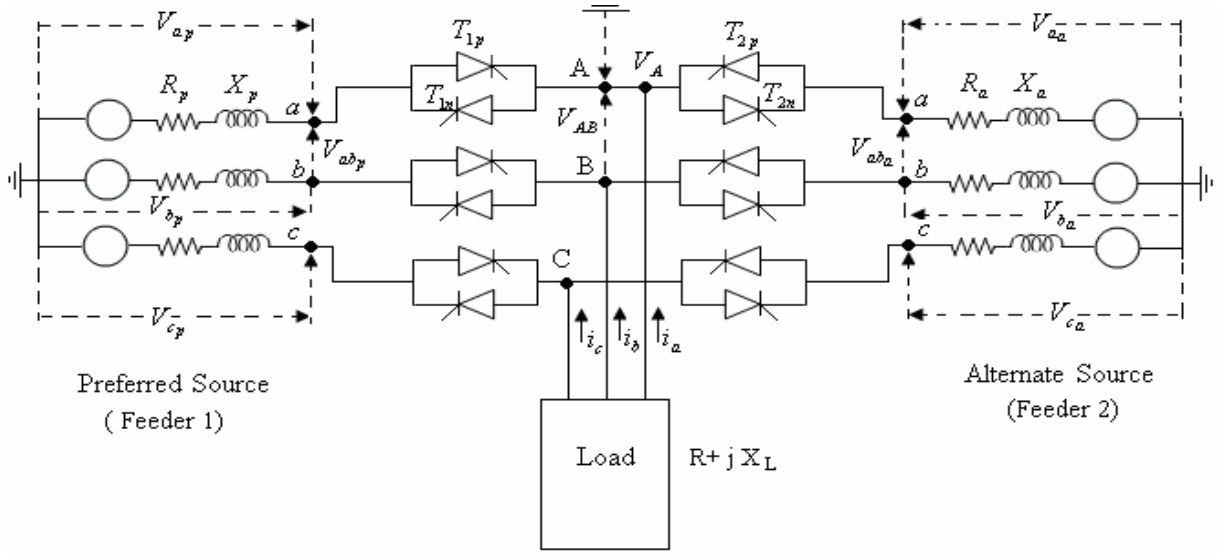

Fig.7: Three Phase STS System with SCR Switching Devices and Configured with R-L Load

3.1 Transfer Time Estimation

Transfer-time estimation of a STS is not a straightforward process due to its dependence on commutation between the thyristor switches in each phase. The commutation process itself is determined by the system parameters and the component characteristics. The following realistic assumptions are made to make the estimation task manageable.

• Preferred and alternate sources are in-phase. This is a realistic assumption for practical distribution systems.

• Voltage drops across the thyristors are negligible with respect to the system voltage.

• Line impedances are negligible compared to the Load impedance.

• No cross current flows during the transfer process.

Considering the above assumptions, transfer time is analytically estimated for RL loads under various fault/disturbance conditions. If the incoming thyristor, e.g., T_{2p} of Fig.7, is negatively biased when a disturbance is detected, commutation fails. In this case, the line current in the corresponding phase decays as a function of the system parameters, e.g., the load power factor and the fault conditions. Commutation begins when a voltage zero-crossing is reached and the incoming thyristor is forward biased. The following subsections describe the procedure of estimating the transfer time in case of symmetrical and asymmetrical disturbances.

1. Three-Phase Under-Voltage Disturbances

If a three-phase under-voltage disturbance occurs in the preferred source and commutation between the incoming and outgoing thyristors of only phase-a fails, from Fig.7, one deduces;

$$V_{a_p} - V_{b_a} = R_l(i_a - i_b) + L_l\left(\frac{di_a}{dt} - \frac{di_b}{dt}\right) \quad (5)$$

$$V_{a_p} - V_{c_a} = R_l(i_a - i_c) + L_l\left(\frac{di_a}{dt} - \frac{di_c}{dt}\right) \quad (6)$$

$$i + i_b + i_c = 0 \quad (7)$$

Where i_a, i_b and i_c are the load currents. Solving (5)–(7) for i_a yields

$$\frac{di_a}{dt} + \frac{1}{\tau_l} i_a = \frac{2V_{ap} + V_{aa}}{3L_l}; \tau_l = \frac{L_l}{R_l} \quad (8)$$

The preferred and alternate sources are in-phase; therefore, if u is the percentage of under voltage during the transfer process, then

$$V_{a_a} = \hat{V}_p \cos(\omega t + \phi) \quad (9)$$

and

$$V_{a_p} = \left(1 - \frac{u}{100}\right)\hat{V}_p \cos(\omega t + \phi) \quad (10)$$

Where $\hat{V}_p$ the peak is value of phase voltage, ω frequency, and ϕ is the initial angle. From *(8), (9)* and *(10),* i_a is deduced

$$i_a(t) = (i_{ao} - K_m \cos(\phi - \xi))e^{t/\tau_l} + K_m \cos(\omega t + \phi - \xi \quad (11)$$

where i_{ao} is phase-a current when load transfer begins, ξ is the load angle
and

$$K_m = \frac{\hat{V}_p(1+2u)}{3\sqrt{R_l^2 + (\omega L_l)^2}} \quad and \quad \xi = \tan^{-1}\left(\frac{\omega L}{R_l}\right) \quad (12)$$

Transfer time is found by solving (11) for $i_a(t)=0$. The maximum transfer time occurs when the transfer process begins at a voltage zero-crossing. Load transfer is completed at the next current zero-crossing. It is observed that with the increase of the percentage of under voltage, the transfer time increases and the total load-transfer time decreases. The decrease in the total load-transfer time is due to the fact that more severe voltage drops are detected faster, thus decreasing the detection time. The results also show that at higher load power factor, the transfer time is shorter.

2. Single-Phase-To-Ground Fault

When a single-phase-to-ground fault is detected, if the alternate-source phase voltage and the preferred-source line current direction corresponding to the faulty phase have the same polarity, commutation occurs and the transfer time is negligible. Otherwise commutation fails, and the transfer time will be determined by the current zero-crossing. If phase-a is the faulty phase, then from (11) and for $u=0$, i_a can be found from

$$i_a(t) = (i_{ao} - K_m \cos(\phi - \xi))e^{t/\tau_l} + K_m \cos(\omega t + \phi - \xi \quad (1$$

where i_{ao} is phase-a line current at the instant of fault/disturbance detection, ξ is the load angle, and

$$K_m = \frac{\hat{V}_p}{3\sqrt{R_l^2 + (\omega L_l)^2}}$$

For some cases, e.g., $0 < \phi < 30°$, the transfer time is only the commutation time which can be neglected. The transfer time in the case of loads with a power factor of 0.8 or 0.9 is also negligible. The reason is that the polarities of the corresponding phase voltage and line current are the same at the instant of fault detection resulting in a successful commutation.

3. Phase-To-Phase Fault

From Fig.7, if a phase-to-phase fault occurs between phase-a and phase-b of the preferred source, the equations expressing line currents are

$$L_l \frac{di_a}{dt} + R_l i_a = \frac{1}{3}(2V_{AB} + V_{BC}) \qquad (14)$$

$$L_l \frac{di_b}{dt} + R_l i_b = \frac{1}{3}(V_{BC} + V_{AB}) \qquad (15)$$

where V_{AB} and V_{BC} are the load line voltages, and i_a and i_b are phase-a and phase-b line currents. During the fault period

$$V_A = V_B = \frac{1}{2}(V_{a_a} + V_{b_a}) \text{ and } V_C = V_{c_a} \qquad (16)$$

Therefore, during the detection process

$$L_l \frac{di_a}{dt} + R_l i_a = -\frac{1}{2}V_{c_a} \qquad (17)$$

$$L_l \frac{di_b}{dt} + R_l i_b = -\frac{1}{2}V_{c_a} \qquad (18)$$

Solving (17) and (18) for i_a and i_b yields:

$$i_a(t) = (i_{ao} - K_m \cos(\phi + 120^\circ - \xi))e^{-t/\tau_l} + K_m \cos(\omega t + \phi + 120° - \xi) \qquad (19)$$

$$i_b(t) = (i_{bo} - K_m \cos(\phi + 120^\circ - \xi))e^{-t/\tau_l} + K_m \cos(\omega t + \phi + 120° - \xi) \qquad (20)$$

where i_{ao} and i_{bo} are phase-a and phase-b currents at the fault instant, and

$$K_m = -\frac{\hat{V}_p}{2\left(\sqrt{R_l^2 + (L_l\omega)^2}\right)} \qquad (21)$$

When a fault is detected, depending on the load voltage and current, commutation may or may not occur. If phase-b is transferred to the alternate source at t_2, phase-a is transferred at t_3 and $t_3 > t_2$, since $V_B = V_{b_a}$, then during $t_2 < t < t_3$ from (14):

$$L_l \frac{di_a}{dt} + R_l i_a = -\frac{3}{4}V_{c_a} \qquad (22)$$

and phase-a current is

$$i_a(t) = (i'_{ao} - K_m \cos(\phi + 120° - \xi))e^{-t/\tau_l} + \mathrm{K_m} \cos(\omega t + \phi + 120° - \xi) \qquad (23)$$

where

$$i'_{ao} = (i_{ao} - K_m \cos(\phi + 120° - \xi))e^{-t2/\tau_l} + \mathrm{K_m} \cos(\omega t_2 + \phi + 120° - \xi)$$

and

$$K_m = -\frac{3\hat{V}_p}{4\left(\sqrt{R_l^2 + (L_l\omega)^2}\right)}$$

Equation (23) is used to obtain the transfer time. In some cases, e.g., $150° < \phi < 180°$, the transfer time is only the commutation time which is negligible. The above analysis is in reference to SCR based STS systems and suggests dependence of transfer time on type of disturbance. In case of STS systems with SCR switching devices the transfer time is significant as compared to STS systems configured with GTO switches [8]. Further the control of SCR based STS system seems to be complex rather than GTO based STS.

4 Simulations Results and Analysis

Extensive simulations were carried out to analyze the performance of detection scheme. The detection scheme of three phase STS system is subjected to various types of disturbances initiated at (1) same time and (2) at different time instants and further the performance of detection scheme is also investigated against switching transients. A tolerance value of 10% has been considered for entire simulation studies.

(1) Impact of disturbance on performance of detection scheme:

(a) Comparison of detection time on basis of type of disturbance and its severity level:

The three-phase STS system is subjected to various single phase, two-phase and three-phase disturbances occurring at same point-on-wave and the variations in detection time are investigated.

The detection time for three-phase sag/swell events of different magnitudes and each initiated at t= 0.025 sec are shown in Fig.8 (a) to 8(f). Results for the same are tabulated in Table 1.

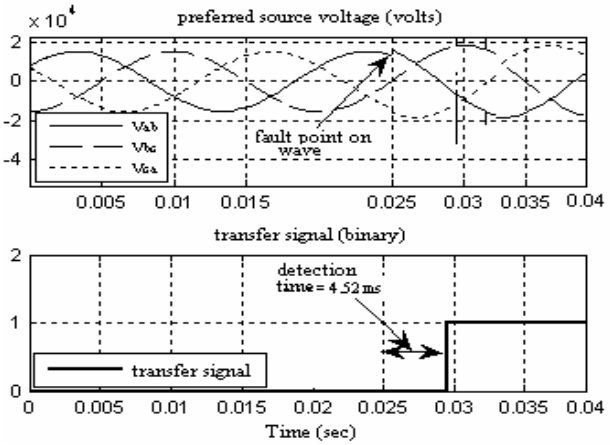

Fig.8 (a): Detection time for 20% swell

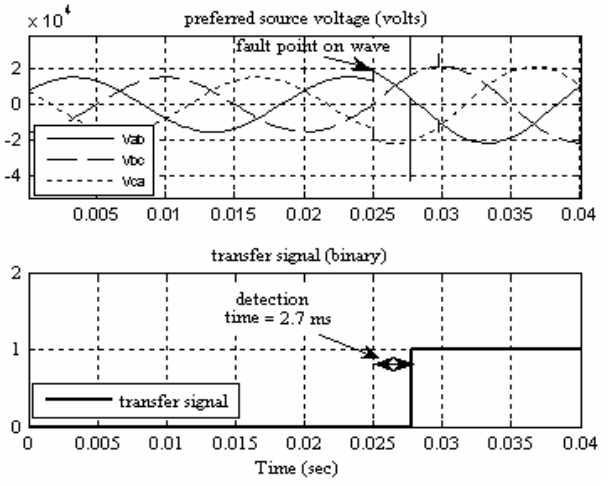

Fig.8 (b): Detection time for 40% swell

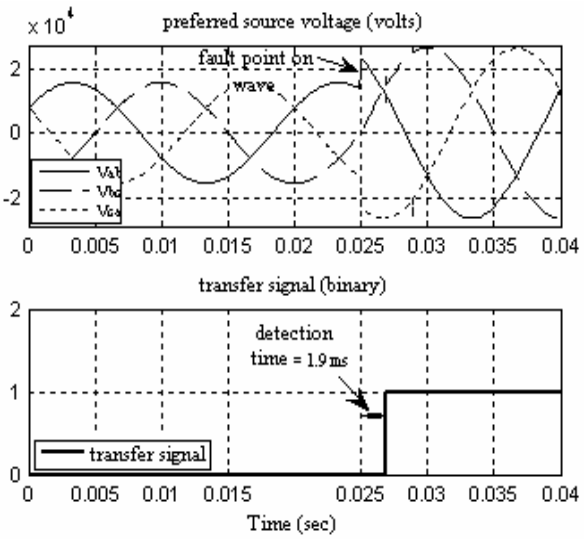

Fig.8 (c): Detection time for 70% swell

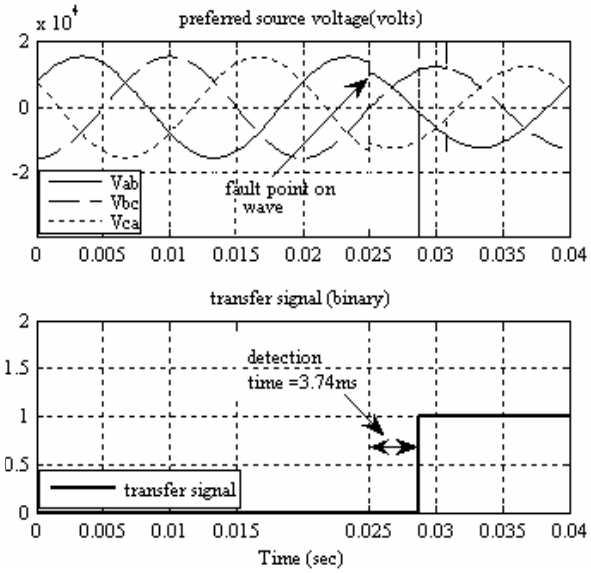

Fig.8 (d): Detection time for 20% sag

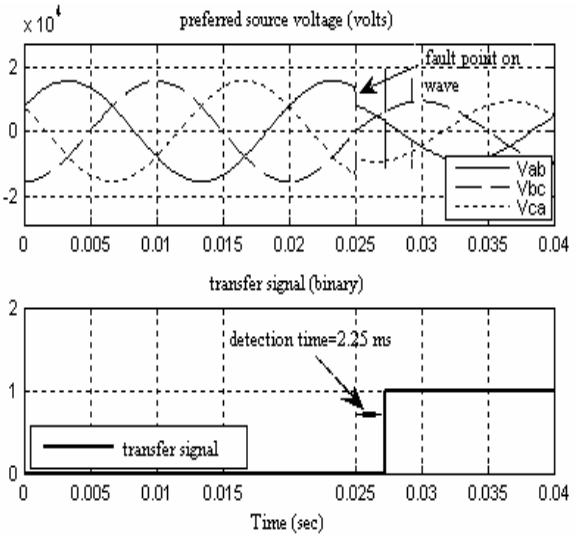

Fig.8 (e): Detection time for 40% sag

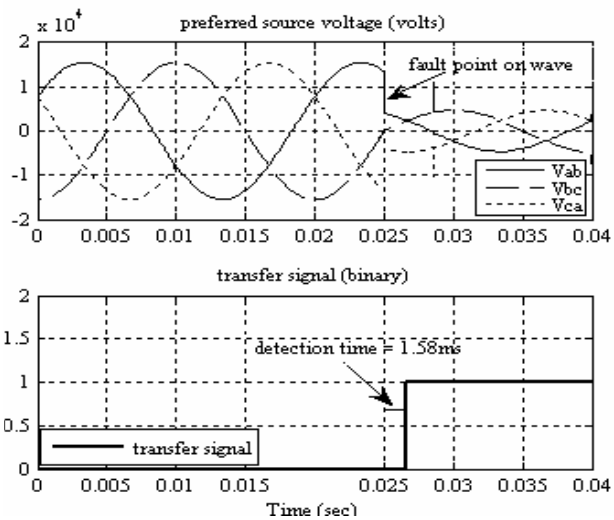

Fig.8 (f): Detection time for 70% sag

Fig.9 (a) to 9(f) shows detection time for two-phase disturbances with severity levels of 20%, 40% &70 %.

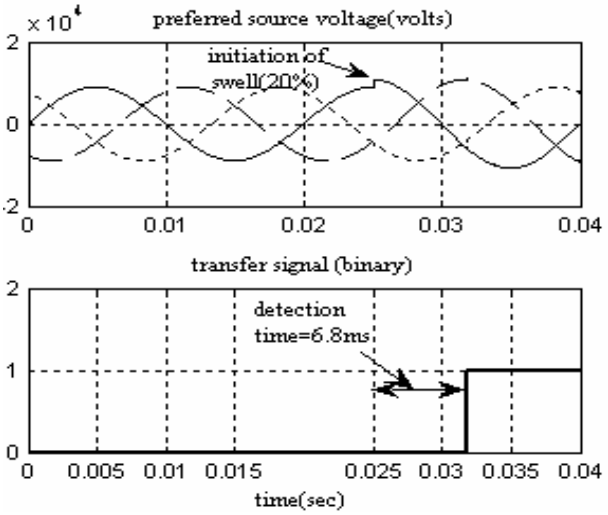

Fig.9 (a): Detection time for two-phase swell of 20%

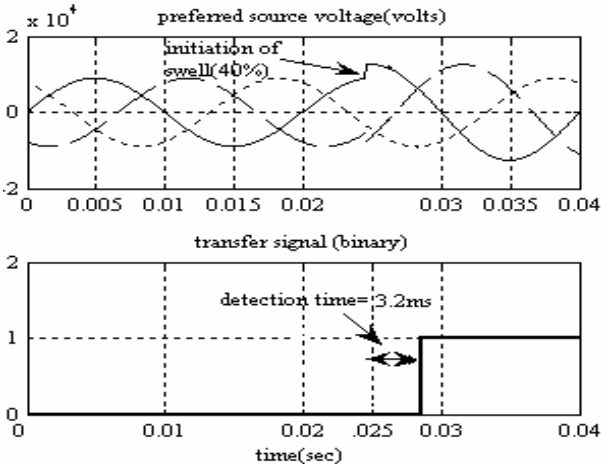

Fig.9 (b): Detection time for swell of 40%

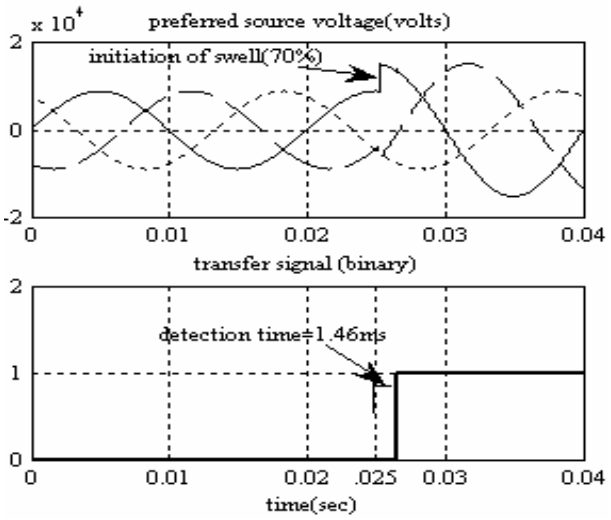

Fig.9 (c): Detection time for two-phase swell of 70%

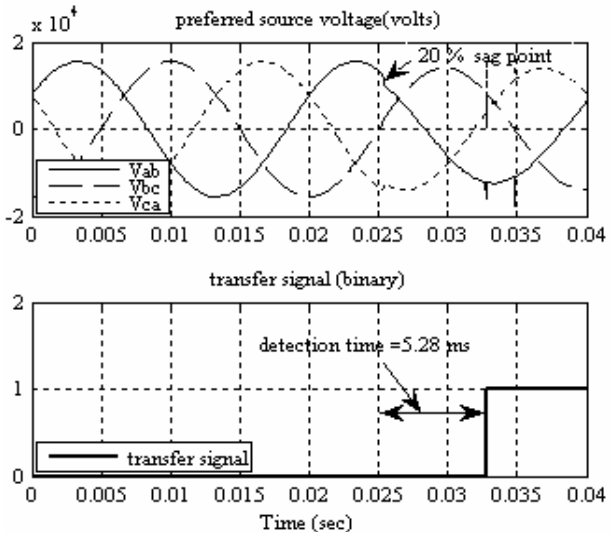

Fig.9 (d): Detection time for two-phase sag of 20%

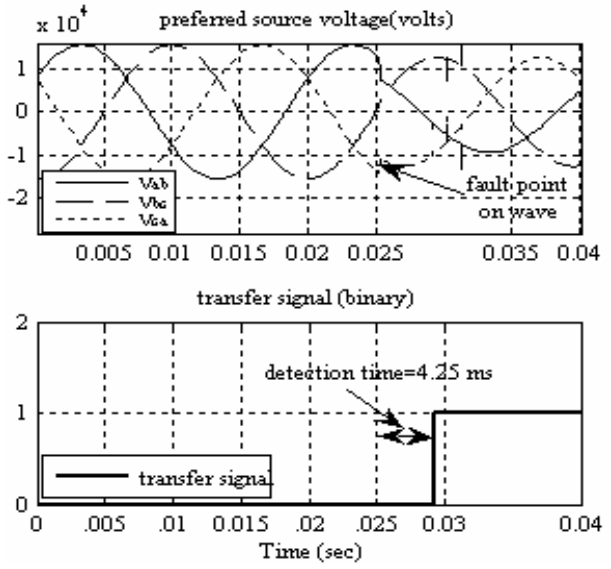

Fig.9 (e): Detection time for two-phase sag of 40%

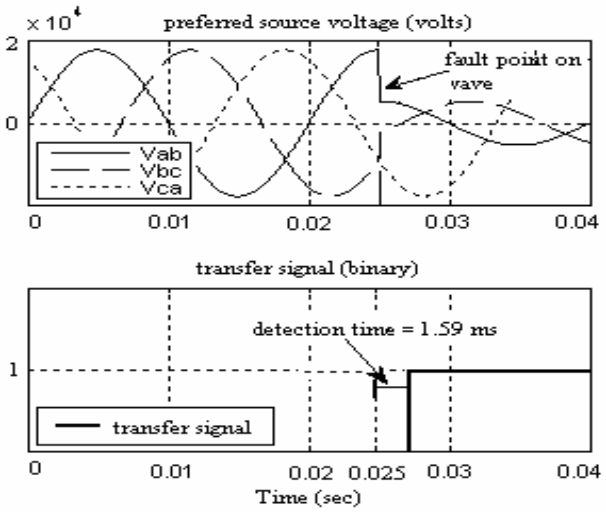

Fig.9 (f): Detection time for two-phase sag of 70%

Fig.10 (a) to 10(f) shows detection time for single phase disturbances of severity levels 20, 40 &70 %.

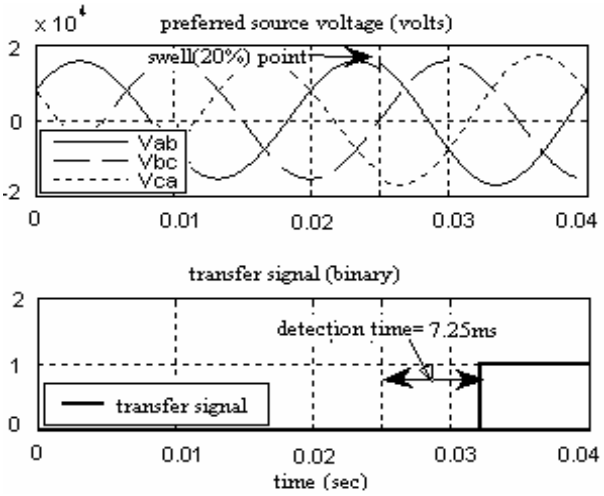

Fig.10 (a): Detection time for single-phase swell of 20%

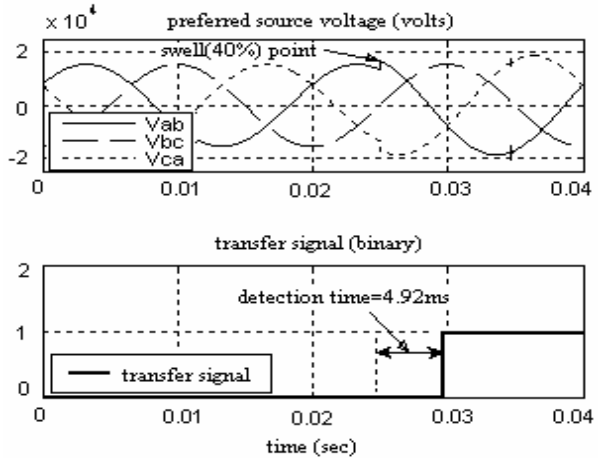

Fig.10 (b): Detection time for single-phase swell of 40%

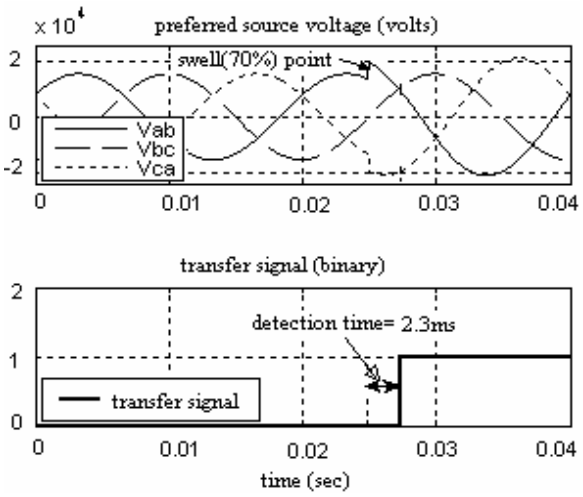

Fig.10 (c): Detection time for single-phase swell of 70%

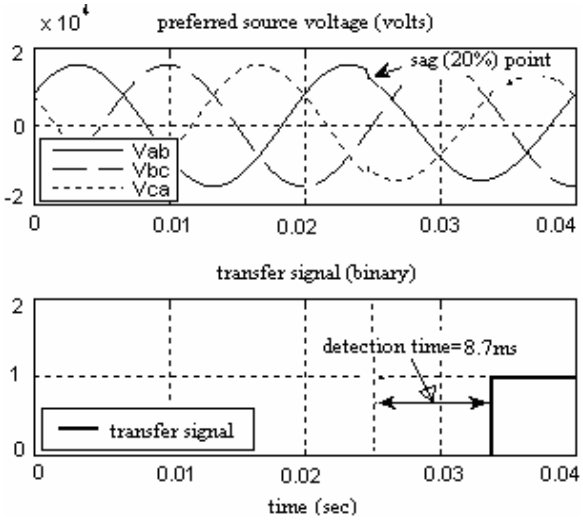

Fig.10 (d): Detection time for single-phase sag of 20%

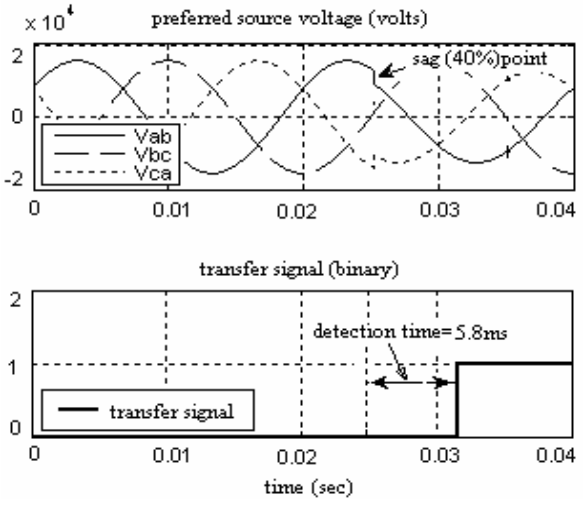

Fig.10 (e): Detection time for single-phase sag of 40%

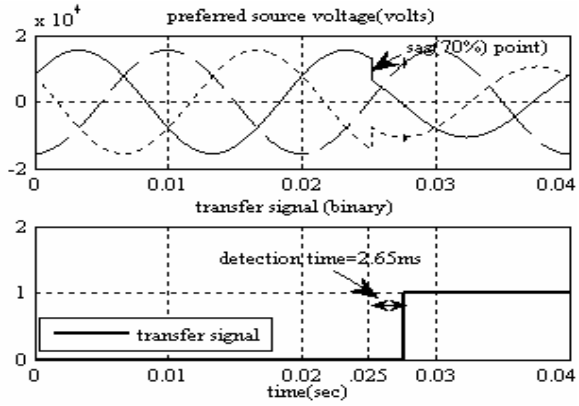

Fig.10 (f): Detection time for single-phase sag of 70%

Table 1: Detection time for various disturbances

S.no.	Disturbance Type (2-ph/3-ph)	Degree of disturbance (%)	Detection time (ms)
1	3-ph swell	20	4.52
2	3-ph swell	40	2.7
3	3-ph swell	70	1.9
4	3-ph sag	20	3.74
5	3-ph sag	40	2.25
6	3-ph sag	70	1.58
7	2-ph swell	20	6.8
8	2-ph swell	40	3.2
9	2-ph swell	70	1.46
10	2-ph sag	20	5.28
11	2-ph sag	40	4.25
12	2-ph sag	70	1.59
13	1-ph swell	20	7.25
14	1-ph swell	40	4.92
15	1-ph swell	70	2.30
16	1-ph sag	20	8.7
17	1-ph sag	40	5.8
18	1-ph sag	70	2.65

(B) Comparison of detection time based on the point-on-wave where disturbance has initiated:

The detection scheme is subjected to different magnitude single-phase sags occurring at different instants (point-on-wave).Characteristics shown in Fig.11 describes the variations in detection time for various single-phase disturbances initiated at different points-on-wave.

(2) Impact of transients on performance of detection scheme:

Here the impact of switching transients on detection scheme is analyzed. Transients may appear either due to switching of STS devices itself or due to switching of large loads and their effect may propagate into the sensor elements of detection scheme and may mislead to a faulty transfer.Fig.12 (a) and Fig.12 (b) shows the relevant waveforms.

One of the rather common solutions to this problem is to use a suitable filter. But limitation of filter circuit arises for events having disturbance magnitude very close to the tolerance levels adopted in detection scheme. In such a case the impact of transients on detection scheme becomes critical and there is a possibility this may interpreted as a voltage recovery, leading to faulty transfer of load back to the unhealthy preferred source.

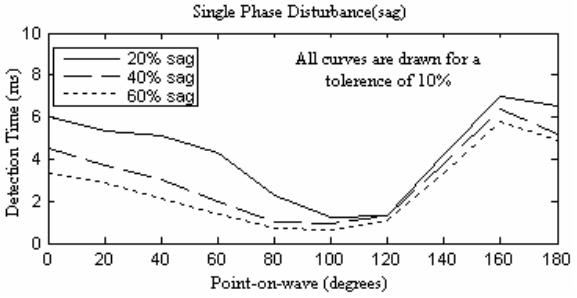

Fig.11: Variations in detection time with respect to disturbances initiated at different points-on-wave

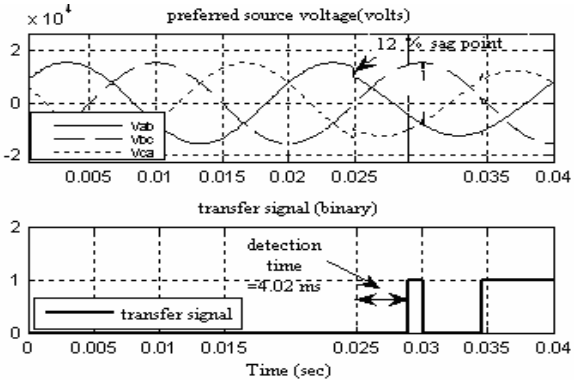

Fig.12: (a) Flaw in detection (transient interpreted as voltage recovery in source)

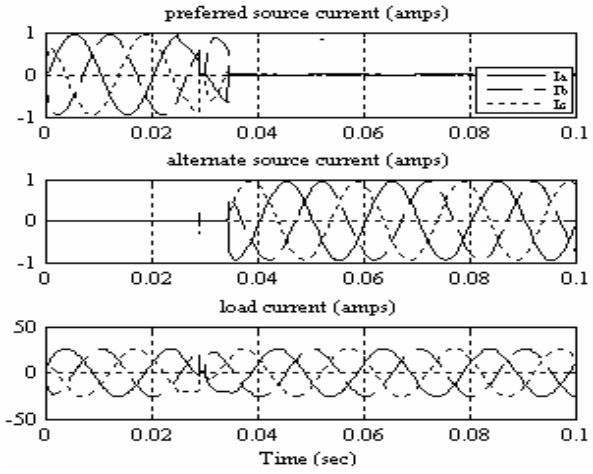

Fig.12: (b) Load transferred back to unhealthy preferred source

To overcome this situation a modification is proposed in the existing detection scheme (as shown in Fig.13 (a) so as to decrease the sensitivity of the scheme against such transients. Once a transfer

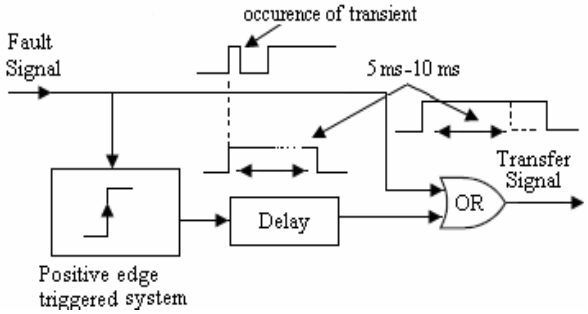

Fig.13 (a): Modified detection scheme

is initiated a sufficient delay (nearly 5 ms depending upon the power quality need of a specific sensitive load) must be ensured before a transfer of load back to the preferred source. By employing an appropriate delay pattern, ambiguous transfer leading to significant interruption can be avoided. Fig.13 (b) shows the improved results for same event after incorporating the modifications in the existing detection scheme.

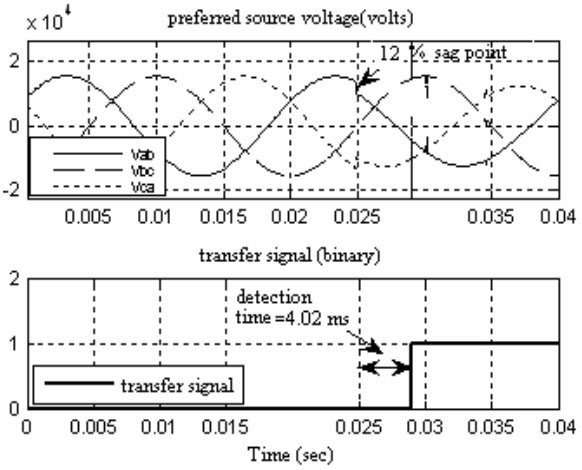

Fig.13: (b) Precise detection of disturbance

5 Conclusions

In this paper the performance of detection scheme has been analyzed against various types and degree of disturbances arising in supply system. Detection time for different events with different severity levels along with their occurrences at same and different instants has been calculated. It is found that more severe is the event less is the detection time. Moreover sag/swells of same magnitude lead to different detection times depending upon the instant or point-on-wave at which the disturbance is initiated. Furthermore simulation analysis suggests that the impact of switching transients on the performance of STS system can be considerably reduced by employing the modified detection scheme. In addition to this it was observed that choice of filter order and damping ratio has significant effect on performance of detection scheme. A higher damping ratio results in fast detection of disturbances but at the same time the control scheme becomes more prone to transients whereas lower values may lead to sluggish response of control scheme leading to delayed detection.

References:

[1] M.N. Moschakis and N. D. Hatziargyroiu, A Detailed Model for a Thyristor Based Static Transfer Switch, *IEEE Transactions on Power Delivery, Volume: 18, Issue: 4,* Oct. 2003, pp. 1442 - 1449.

[2] H. Mokhtari, S.B. Dewan, M.R. Iravani, Benchmark Systems for Digital Computer Simulation of A Static Transfer Switch, *IEEE Transactions on Power Delivery, Volume: 16, Issue: 4* October-2001, pp. 724 - 731.

[3] H. Mokhtari, S.B. Dewan, M.R. Iravani, Performance Evaluation of Thyristor Based Static Transfer Switch, *IEEE Transactions on Power Delivery, Volume: 15*, July 2000, pp. 960 -966.

[4] A. Sannio, Static Transfer Switch: Analysis of Switching Conditions and Actual Transfer Time, *IEEE Power Engineering Society Winter Meeting*, Columbus, Ohio, 2001.

[5] H. Mokhtari, S.B. Dewan, M.R. Iravani, Analysis of a Static Transfer Switch With Respect to Transfer Time, *IEEE Transactions on Power Delivery, Volume: 17, Issue: 1,* 2002, pp. 190 -199.

[6] H. Mokhtari, M.R. Iravani, Impact of Difference of Feeder Impedances on the Performance of a Static Transfer Switch, *IEEE Transactions on Power Delivery, Volume: 19 Issue: 2,* 2004, pp.679-685.

[7] R. K. Pachar, H. P. Tiwari, Performance Evaluation of Static Transfer Switch, *WSEAS Transactions on Systems and Control*, *Issue 3, Volume 3,* March 2008, pp 137-148.

[8] R. K. Pachar, H. P. Tiwari, N. Jhajharia, S. L. Surana, Simulation Study of GTO Based Static Transfer Switch Using MATLAB, *6th WSEAS International Conference on CSECS*, Cairo, Egypt, Dec-2007, pp. 264-269.

[9] Hu Guo-Sheng, Ren Guang Yong, Jiang Jin-Jian, Power Quality Faint Disturbance Identification Using WPEE and WSVMs, *WSEAS Transactions on Power Systems, Volume:2, Issue:7,*July 2007, pp. 1625-1639

[10] Maha Sharkas, A Combined DWT and DCT with PCA for Face Recognition, *WSEAS Transactions on Systems, Volume:4, Issue: 10,*October 2005, pp. 1707-1734.

[11] R.C. Berredo, L.N. Canha, P.Ya. Ekel, L C.A. Ferreira and M.V.C. Maciel, Experimental Design and Models of Power System Optimization and Control, *WSEAS Transactions on Systems and Control, Volume: 3*, *Issue: 1*, January 2008, pp. 40-49.